A Theory of the Mean Flow Driven by Long Internal Waves in a Rotating Basin, with Application to Lake Kinneret

HSIEN WANG OU

Joint Program in Physical Oceanography, Massachusetts Institute of Technology, Woods Hole Oceanographic Institution, Woods Hole, MA 02543

JOHN R. BENNETT

Environmental Research Laboratories, Great Lakes Environmental Research Laboratory, NOAA, Ann Arbor, MI 48104

(Manuscript received 17 April 1978, in final form 25 July 1979)

ABSTRACT

The rectified flow induced by wind-driven internal seiches in a rotating lake is studied. Friction and nonlinearity combine to generate a secondary mean flow which is calculated analytically for the case of a uniform depth lake and numerically for variable depth.

The theory is applied to Lake Kinneret, the former Sea of Galilee, where the diurnal wind forcing produces a large internal Kelvin wave and which has a strong cyclonic mean flow. The uniform depth model reproduces the diurnal response adequately, but variable depth is required to reproduce the mean flow.

1. Introduction and summary

This theory was motivated by Serruya's (1975) observation that in summer Lake Kinneret circulates cyclonically. This is commonly observed in other lakes (Emery and Csanady, 1973) and a number of mechanisms have been proposed to explain it. Because Lake Kinneret is small, one would not expect the simplest mechanism, a wind stress curl, to be significant. Because it is shallow, it is not as likely that the spring thermal circulation would persist long into summer. The presence of large-amplitude internal Kelvin waves driven by a predominantly diurnal wind leads us to speculate that the mean flow is a residual flow due to nonlinearity associated with either the advective terms or the large fluctuations of the thermocline depth.

One mechanism by which nonlinearity can generate a mean flow has been advanced by Wunsch (1973). He found that the Lagrangian mean flow induced by the first mode internal Kelvin wave is cyclonic near the surface and bottom, but anticyclonic at mid-depth. The Eulerian mean flow, however, is assumed zero in his model. As it is precisely this Eulerian mean flow which is measured by a fixed current meter, his model cannot explain Serruya's observations. The Stokes drift that he calculated is mostly a kinematic result of the wave field, but the existence of an Eulerian mean flow requires a dynamical balance of the second order. It is this dynamical balance we try to pursue here. Since the Lagrangian mean is the sum of Eulerian mean and Stokes drift (Longuet-Higgins, 1969), Wunsch's work can be regarded as a complement to the present work if the Lagrangian mean is to be calculated.

In a different context, Thompson (1970) studied the Eulerian mean flow generated by periodic motions in a rotating cylinder. He found, in the inviscid interior, that the azimuthal mean flow is indeterministic; it is through the bottom Ekman layer where friction is important that this degeneracy is removed.

Similarly, for our theory, friction is essential; but the exact shape of the lake and the exact time and space variations in the wind are not essential. Thus, it is sufficient to consider a two-layer circular lake driven by a uniform wind periodic in time. We will allow the depth of the lake to be at most a function of radius and will only use linear bottom and interface friction. The basic equations for this model are given in Section 2.

In Section 3, before the full model is considered, a simple analytical example is given to bring out some of the essentials of the underlying physics with a minimum of mathematics. This analysis considers a constant depth, homogeneous ocean bounded on one side by a straight coast, and driven by a longshore wind propagating along the coast. The flow is assumed to consist of a primary or first-order flow driven by the wind and obeying the linearized equations; and a secondary mean flow, averaged in time or the longshore direction, driven by the nonlinear terms.

0022-3670/79/061112-14$07.50

From the vorticity equation, it is shown that the nonlinear mechanisms which account for the residual flow can be classified into two categories. One is associated with correlation between surface elevation and either the surface or bottom stress, and will be referred to as the feedback mechanism. The other is associated with the flux of perturbation potential vorticity, and hence will be referred to as the advective mechanism. Friction is essential for both mechanisms, for without friction many of the important correlations of primary variables are zero and the potential vorticity perturbation is zero. It is shown that the advective process cannot generate any mean flow at the coast and that the longshore mean flow must have reversals in direction. The mean longshore flow at the coast is found to be in the same direction as a free Kelvin wave propagates. Its amplitude decreases offshore and has at least one zero crossing before eventually decaying to zero. These results have their parallels in the circular basin case.

In Section 4 the case of a two-layer circular basin with a flat bottom is also treated by analytical methods. Although complicated by stratification and the circular geometry, the basic nonlinear mechanisms are the same. In particular, it is shown that a mean circulation at the shore can only be generated by the feedback mechanism, and that the mean azimuthal flow in the lower layer must have reversals in direction so that the net bottom torque vanishes. The signs of the lower layer flow, the vertical shear and the thermocline displacement at the coast are determined analytically. It is found that the lower layer flow is cyclonic near the shore when the forcing frequency is lower than some critical value. Since a free Kelvin wave has a frequency below this critical value, we conclude that the lower layer flow at the coast is generally cyclonic if the Kelvin mode is the dominant mode that is excited. The sign of vertical shear at the coast, however, depends on more parameters and no such simple conclusion can be drawn for the general case. But for the special case of a resonant Kelvin mode, this vertical shear is found to be cyclonic if δ (the ratio of bottom friction coefficient to interface friction coefficient) is smaller than some critical value δ_c. Contours of δ_c are plotted as a function of dimensionless parameters measuring stratification (Δ) and mean thermocline depth (λ). The critical value of λ, above which no cyclonic vertical shear is possible, is found to be approximately ⅓ for $\Delta = 2$, and approaches ½ as Δ approaches infinity (i.e., the radius of lake becomes much larger than its internal Rossby deformation radius). The sign of mean thermocline displacement is closely related to the sign of the vertical shear. It is found that whenever the thermocline is deeper than half the total depth, there is an anticyclonic vertical shear and an upwelling at coast, and a cyclonic vertical shear is always accompanied by a downwelling at coast.

In Section 5 the theory is applied to Lake Kinneret (formerly the Sea of Galilee), a lake of relatively simple shape which is driven by a regular diurnal wind. The primary response predicted by the theory agrees favorably with the observations. But, for the secondary mean field, the agreement is not as satisfactory.

In Section 6 the numerical model of Bennett (1978), which includes bottom topography, is used to calculate the mean barotropic flow and thermocline shape over the whole basin. These calculations show that the comparison with observation is greatly improved if the lake has a parabolic bottom. The mean coastal upwelling zone of the constant depth model is pushed offshore, while an apparent downwelling takes place right at the coast. This implies a cyclonic vertical shear and hence better agreement with observations. In addition, the numerical model is able to reproduce the intense upwelling zone at the northwest corner of the lake, and the maximum mean current in the northwest and southeast quadrants.

As all the major features of the secondary mean fields have been reproduced by this model, it is suggested that the mean flow observed is caused by the nonlinear mechanisms discussed earlier. More work, however, is needed to understand these mechanisms in a lake of variable depth.

2. Basic equations

We will use the hydrostatic, Boussinesq and rigid-lid approximations. Using the notation of Fig. 1, the governing equations are

$$\left.\begin{aligned}
&\frac{\partial \mathbf{V}_1}{\partial t} + \mathbf{V}_1\cdot\nabla\mathbf{V}_1 + f\hat{\mathbf{k}}\times\mathbf{V}_1 = -g\nabla\eta + \frac{\mathbf{F} - C_I(\mathbf{V}_1 - \mathbf{V}_2)}{h}\\
&\frac{\partial \mathbf{V}_2}{\partial t} + \mathbf{V}_2\cdot\nabla\mathbf{V}_2 + f\hat{\mathbf{k}}\times\mathbf{V}_2 = -g\nabla\eta + g'\nabla h + \frac{C_I(\mathbf{V}_1 - \mathbf{V}_2) - C_B\mathbf{V}_2}{D - h}\\
&\frac{\partial h}{\partial t} + \nabla\cdot[h\mathbf{V}_1] = 0\\
&\nabla\cdot[h\mathbf{V}_1 + (D - h)\mathbf{V}_2] = 0
\end{aligned}\right\}. \tag{2.1}$$

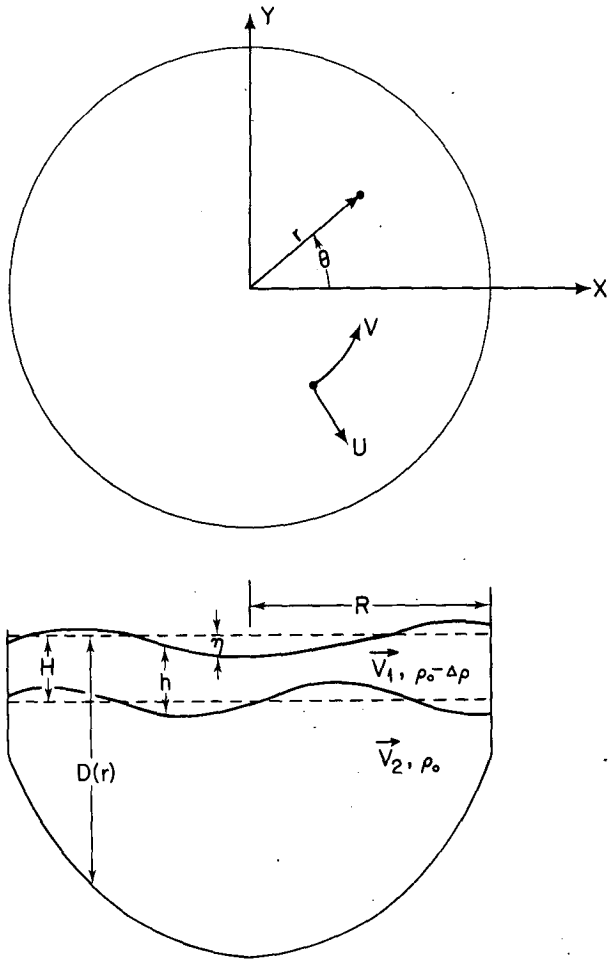

FIG. 1. Definition of variables for a two-layer circular lake model.

The first two are momentum equations for the upper and lower layers; the last two are continuity equations. The boundary conditions are that the normal component of the current is zero at the shore and that there is no singularity at the center.

F is the wind stress, assumed to be spatially uniform, C_I and C_B are linear interface and bottom friction coefficients, $g' = g(\Delta\rho/\rho_0)$ is the reduced gravity and η is the free surface displacement.

We define the baroclinic and barotropic velocities as

$$\left.\begin{aligned} \mathbf{V} &= \mathbf{V}_1 - \mathbf{V}_2 \\ \underline{\mathbf{V}} &= \frac{h}{D}\mathbf{V}_1 + \left(1 - \frac{h}{D}\right)\mathbf{V}_2 \end{aligned}\right\} . \tag{2.2}$$

For the numerical model of Section 6, these equations are solved in above dimensional form. For the rest of the analytical theory, the depth D will be assumed to be constant and the equations will be nondimensionalized as follows:

$$r \to Rr \quad (R \text{ is the radius of the basin}),$$

$$t \to f^{-1}t,$$

$$(\mathbf{V}_1,\mathbf{V}_2) \to (\mathbf{V}_1,\mathbf{V}_2)\frac{F^*(1-\lambda)}{fH},$$

$$(\mathbf{V},\underline{\mathbf{V}}) \to \left(\frac{1}{1-\lambda}\mathbf{V},\underline{\mathbf{V}}\right)\frac{F^*(1-\lambda)}{fH},$$

$$h \to H(1 + \Delta\epsilon h),$$

$$\mathbf{F} \to F^*\mathbf{F},$$

$$\eta \to \frac{\eta RF^*(1-\lambda)}{gH},$$

where

F^* wind stress amplitude

λ ratio of mean thermocline depth to total depth $[=H/D]$

ϵ a Rossby number $[=F^*(1-\lambda)/f^2\mathrm{RH}]$

Δ square of the ratio of the basin radius to the internal Rossby radius of deformation $[=R^2f^2/g'D\lambda(1-\lambda)]$.

We will assume that ϵ is small, then the dimensionless governing equations correct to $O(\epsilon^2)$ in terms of baroclinic and barotropic modes are

$$\left.\begin{aligned} &\frac{\partial \mathbf{V}}{\partial t} + \hat{\mathbf{k}} \times \mathbf{V} \\ &= -\nabla h + \mathbf{F} - \alpha_I\mathbf{V} + \alpha_B\mathbf{V}_2 - \epsilon\left\{\mathbf{V}\cdot\nabla\underline{\mathbf{V}} + \underline{\mathbf{V}}\cdot\nabla\mathbf{V} + \frac{1-2\lambda}{1-\lambda}\mathbf{V}\cdot\nabla\mathbf{V} + \Delta h\mathbf{F} - \Delta\right. \\ &\left.\times\left[\frac{\alpha_I(1-2\lambda)}{1-\lambda} - \frac{\alpha_B\lambda^2}{(1-\lambda)^2}\right]h\mathbf{V} - \frac{\alpha_B\lambda}{1-\lambda}\Delta h\underline{\mathbf{V}}\right\} \Delta\frac{\partial h}{\partial t} + \nabla\cdot\mathbf{V} = -\epsilon\Delta\left[\frac{1-2\lambda}{1-\lambda}\nabla\cdot h\mathbf{V} + \nabla\cdot h\underline{\mathbf{V}}\right] \\ &\frac{\partial \underline{\mathbf{V}}}{\partial t} + \hat{\mathbf{k}} \times \underline{\mathbf{V}} = -\nabla(\eta - h) + \frac{\lambda}{1-\lambda}F - \alpha_B\mathbf{V}_2 \\ &\qquad - \epsilon\left[\frac{\lambda}{1-\lambda}(\Delta h\nabla h + \mathbf{V}\nabla\cdot\mathbf{V} + \mathbf{V}\cdot\nabla\mathbf{V}) + \underline{\mathbf{V}}\cdot\nabla\underline{\mathbf{V}}\right], \qquad \nabla\cdot\underline{\mathbf{V}} = 0 \end{aligned}\right\} \tag{2.3}$$

The two friction parameters

$$\alpha_I = C_I/fD(\lambda - \lambda^2),$$

$$\alpha_B = C_B/fD,$$

are assumed to be in the range $\epsilon \ll \alpha_I, \alpha_B \ll 1$. The dimensionless variables are expanded in a power series of ϵ:

$$h_{\text{total}} = h_0 + \epsilon h_1 + O(\epsilon^2). \quad (2.4)$$

The zero- and first-order variables will henceforth be referred to as being primary and secondary, respectively. Only the primary solution and the time-averaged secondary solution will be discussed here.

3. A simple analytical model

Before considering the full problem, it is instructive to study a simple analytical example to bring out some of the essentials of the underlying physics with minimum mathematical complications. As Bennett (1973, 1978) did, we will consider a homogeneous ocean of uniform depth bounded on one side by a straight coast, as shown in Fig. 2. The wind stress field has only a longshore component and propagates along the coast.

The governing equations are given by

$$\mathbf{v}_t + \mathbf{v}\cdot\nabla\mathbf{v} + f\hat{\mathbf{k}} \times \mathbf{v} + g\nabla h = \mathbf{F}/\mathrm{h} - C_B\mathbf{v}/h, \quad (3.1)$$

$$h_t + \nabla\cdot h\mathbf{v} = 0. \quad (3.2)$$

If we multiply (3.1) and (3.2) by h and $\mathbf{v}$, respectively, and add the resultant equations, we obtain

$$(h\mathbf{v})_t + \nabla\cdot(\mathbf{v}h\mathbf{v}) + f\hat{\mathbf{k}} \times h\mathbf{v} + \nabla h^2/2 = \mathbf{F} - C_B\mathbf{v}. \quad (3.3)$$

Taking the time or y average (denoted by angle braces) of the y component of this equation yields

$$C_B\langle v\rangle = -\partial_x\langle huv\rangle, \quad (3.4)$$

i.e., the longshore mean flow is determined by the divergence of the Reynolds stress. For coastal trapped waves, this implies

$$\int_0^\infty \langle v\rangle dx = 0, \quad (3.5)$$

i.e., any nontrivial longshore mean flow must have reversals in direction. This is a trivial result, if we realize that since the fluctuating wind cannot exert any net force on the flow, the net bottom stress must vanish. As this bottom stress is proportional to the flow, the net longshore flow must therefore vanish. It is also clear from this argument that (3.5) holds even for a variable bottom.

By taking the time average of the vorticity equation, we derive

$$\nabla\cdot\langle\zeta\mathbf{v}\rangle + f\nabla\cdot\langle\mathbf{v}\rangle = \hat{\mathbf{k}}\cdot\nabla \times \langle\mathbf{F}/h - C_B\mathbf{v}/h\rangle, \quad (3.6)$$

where $\zeta \equiv \hat{\mathbf{k}}\cdot\nabla \times \mathbf{v}$ is the relative vorticity.

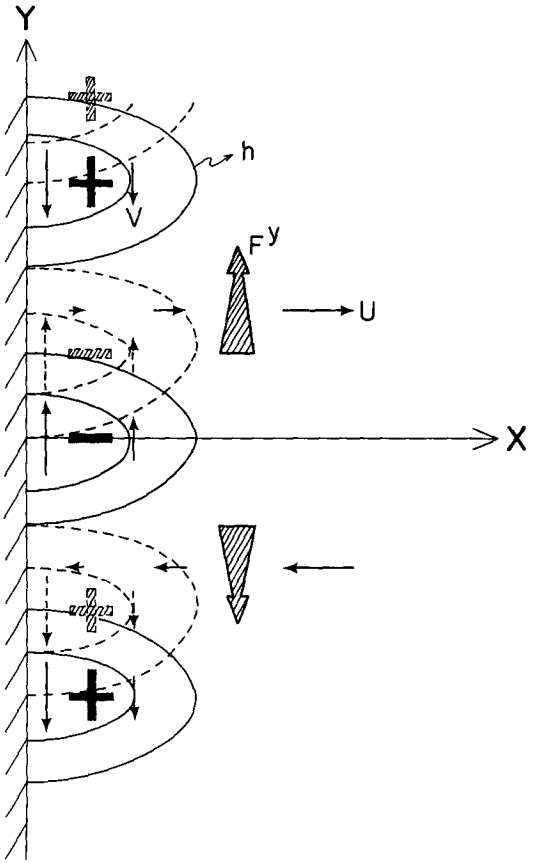

FIG. 2. Primary Kelvin wave driven by longshore wind stress field. Solid contours are surface displacement, solid arrows are velocity and shaded arrows are wind stress. The dashed lines show the wave field with friction.

To proceed further, we assume that

$$h = H(1 + \eta), \quad (3.7)$$

where $\eta \ll 1$ and H is the unperturbed depth. Then (3.2) implies

$$\nabla\cdot\langle\mathbf{v}\rangle = -\nabla\cdot\langle\eta\mathbf{v}\rangle. \quad (3.8)$$

Substituting (3.7) and (3.8) into (3.6), we derive

$$C_B\hat{\mathbf{k}}\cdot\nabla \times \langle\mathbf{v}\rangle = -\nabla\cdot\langle(\zeta - f\eta)\mathbf{v}\rangle + \hat{\mathbf{k}}\cdot\nabla \times \langle C_B\eta\mathbf{v} - \eta\mathbf{F}\rangle. \quad (3.9)$$

Since the first term on the right is the divergence of the flux of potential vorticity, this mechanism will be referred to as the advective mechanism. The second term involves correlation between surface elevation and bottom or surface stress, a mechanism which will be referred to as the feedback mechanism.

Since there is no flux through the boundary, the advective mechanism can only act to redistribute the potential vorticity within the system and cannot generate any net mean vorticity over the entire

domain. Indeed, at the coast, the time average of the y component of (3.1) implies

$$C_B\langle \mathbf{v} \rangle = \langle C_B \eta \mathbf{v} - \eta F^y \rangle, \tag{3.10}$$

i.e., the longshore mean flow at the coast can only be produced by the feedback mechanism. Both these results [(3.5) and (3.10)] have their parallels in the circular basin case.

As an example, to calculate the mean flow from (3.4), we assume that the primary response satisfies the linear dynamics, that the longshore flow is geostrophic, and that the wind stress has only a longshore component. By a scaling similar to that of the previous section, but with a horizontal length scale set equal to the Rossby radius of deformation, the nondimensionalized governing equations for the primary variables are given by

$$-v = -h_x,$$

$$v_t + u = -h_y + F^y - \alpha v,$$

$$h_t + u_x + v_y = 0,$$

where $\alpha \equiv C_B/(fH)$ is a dimensionless frictional coefficient. The boundary conditions are

$$u = 0 \quad \text{at} \quad x = 0,$$

$$h \to 0 \quad \text{as} \quad x \to \infty.$$

With $F^y = e^{i(ly+\sigma t)}$, the solution satisfies

$$h_{xx} - q^2 h = 0,$$

$$h_x + \frac{q^2}{c} h = -\frac{iq^2}{\sigma} F^y \quad \text{at} \quad x = 0,$$

$$h \to 0 \quad \text{as} \quad x \to \infty,$$

where

$$q^2 = \frac{1}{1 - i\dfrac{\alpha}{\sigma}},$$

and $c = \sigma/l$ is the ratio of the longshore phase speed to the free Kelvin wave phase speed. The solution is given by

$$h = Ae^{-qx}, \tag{3.11}$$

where

$$q = \left(1 - i\frac{\alpha}{\sigma}\right)^{-1/2} = \left(1 + \frac{\alpha^2}{\sigma^2}\right)^{-1/4} \exp\left(\frac{i}{2}\tan^{-1}\frac{\alpha}{\sigma}\right), \tag{3.12}$$

$$A = \frac{iq}{\sigma\left(1 - \dfrac{q}{c}\right)} F^y. \tag{3.13}$$

To a first approximation, (3.4) can be written in a dimensionless form as

$$\alpha\langle v \rangle_1 = -\partial_x \langle uv \rangle_0, \tag{3.14}$$

where the subscripts 0 and 1 indicate that the variables within the angle braces are primary and secondary, respectively. At the coast where $u = 0$, we then have

$$\begin{aligned} \alpha\langle v \rangle_1 &= -\langle u_x v \rangle_0 \\ &= \langle h_t h_x \rangle_0 \\ &= \tfrac{1}{2}\,\mathrm{Re}\{-i\sigma A^* \cdot (-qA)\} \\ &= -\tfrac{1}{2}\sigma |A|^2\,\mathrm{Im}\{q\} \\ &< 0. \end{aligned} \tag{3.15}$$

Hence, the mean longshore flow at the coast is always in the same direction a free Kelvin wave propagates regardless of the direction the wind pattern propagates. To understand this physically, consider the inviscid primary wave field illustrated by solid lines in Fig. 2. Without friction the longshore flow and wind stress are necessarily in quadrature, so that there is no work done by the wind. With friction, however, the wave field is shifted as shown by the dashed lines, so that there is a net correlation between wind and longshore flow to balance the dissipation. A positive Reynold stress would then result near shore, and hence a negative longshore flow would be generated at the coast.

To calculate the magnitude of this mean flow at coast, we see that if α/σ is small, then (3.15) implies

$$\langle v \rangle_1 \approx -\tfrac{1}{4}|A|^2 \tag{3.16}$$

which is proportional to the amplitude squared of the primary waves. Thus friction is important even when it is small; given the amplitude of the primary flow, the mean flow is actually independent of the friction coefficient. Substituting (3.13) into (3.16), we obtain another form, giving the mean flow in terms of the wind stress:

$$\left.\begin{aligned} \langle v \rangle_1 &\approx -\frac{|F^y|^2}{4\sigma^2\left(1 - \dfrac{1}{c}\right)^2} && \text{when } c \neq 1 \\ &\approx -\frac{|F^y|^2}{\alpha^2} && \text{when } c = 1 \end{aligned}\right\}.$$

The spatial distribution of $\langle v \rangle_1$ can also be calculated from (3.14), i.e.,

$$\langle v \rangle_1 = -\frac{|F^y|^2}{2\alpha\sigma\left|1 - \dfrac{q}{c}\right|^2} \times \left\{\frac{\alpha}{\sigma}|q|^2 e^{-(q^*+q)x}\,\mathrm{Re}\{q\} - \mathrm{Im}\left[q^*\left(1 - \frac{q}{c}\right)e^{-q^*x}\right]\right\},$$

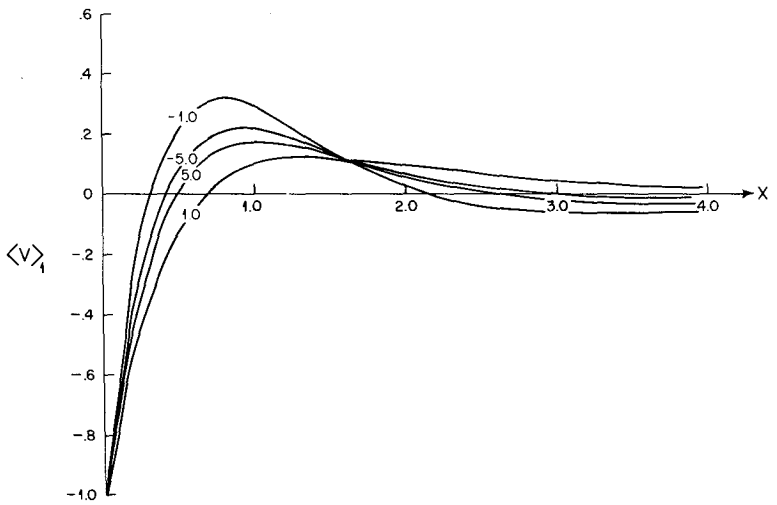

FIG. 3. Profiles of mean longshore flow $\langle v \rangle_1$ for several values of phase speed c. The amplitudes at the coast have been normalized to unity.

which, in the limit α/σ, $\alpha x/\sigma \ll 1$, can be written

$$\langle v \rangle_1 = 2e^{-x}\{(1 - c^{-1})(1 - e^{-x}) - e^{-x} + \tfrac{1}{2}[1 - (1 - c^{-1})x]\},$$

where the amplitude has been normalized to unity at the coast. The profiles of $\langle v \rangle_1$ for several values of c are shown in Fig. 3. The mean longshore flow at the coast is always in the same direction the free Kelvin wave propagates, decreasing in amplitude offshore, with at least one zero crossing somewhere before eventually decaying to zero.

4. Analytical solution of the case of uniform depth

We now consider the full problem of a two-layer circular lake with constant depth, driven by a spatially uniform wind periodic in time. This section is subdivided into two parts, for the primary and secondary response, respectively.

a. The primary response

It is seen, from (2.3), that the primary variables satisfy the O(0) problem:

$$\left.\begin{aligned} &\frac{\partial \mathbf{V}}{\partial t} + \hat{\mathbf{k}} \times \mathbf{V} = -\nabla h + \mathbf{F} - \alpha_I \mathbf{V} + \alpha_B \mathbf{V}_2 \\ &\Delta \frac{\partial h}{\partial t} + \nabla \cdot \mathbf{V} = 0 \\ &\frac{\partial \underline{\mathbf{V}}}{\partial t} + \hat{\mathbf{k}} \times \underline{\mathbf{V}} = -\nabla(\eta - h) + \frac{\lambda}{1 - \lambda}\mathbf{F} - \alpha_B \mathbf{V}_2 \\ &\nabla \cdot \underline{\mathbf{V}} = 0 \end{aligned}\right\}, \tag{4.1}$$

From the vorticity equation for the barotropic flow, it can easily be shown that

$$\underline{\mathbf{V}} = O(\alpha_B).$$

Thus the primary response is baroclinic and satisfies

$$\left.\begin{aligned} &\frac{\partial \mathbf{V}}{\partial t} + \hat{\mathbf{k}} \times \mathbf{V} = -\nabla h + \mathbf{F} - \alpha \mathbf{V} \\ &\Delta \frac{\partial h}{\partial t} + \nabla \cdot \mathbf{V} = 0 \end{aligned}\right\}, \tag{4.2}$$

where $\alpha = \alpha_I + \alpha_B\lambda/(1 - \lambda)$. Any uniform wind with frequency σ can be decomposed into two rotary components, i.e.,

$$\begin{aligned} \mathbf{F} &= 2\hat{\mathbf{i}} \cos\sigma t \\ &= \mathrm{Re}(\hat{\mathbf{r}} + i\hat{\boldsymbol{\theta}})[e^{i(\theta+\sigma t)} + e^{i(\theta-\sigma t)}], \end{aligned}$$

where $\hat{\mathbf{i}}$, $\hat{\mathbf{r}}$ and $\hat{\boldsymbol{\theta}}$ are unit vectors in the x, r and θ directions.

The periodic solutions associated with either the clockwise or counterclockwise component can be written in the form

$$h(r,\theta,t) = \hat{h}(r)e^{i(\theta+\sigma t)}, \tag{4.3}$$

where positive (negative) σ corresponds to clockwise (counterclockwise) component.

The solution of (4.2) is given by

$$\hat{h} = \hat{A}J_1(sr), \tag{4.4}$$

$$\hat{u} = \frac{i\sigma}{\sigma^2 - 1}\left(\frac{\partial \hat{h}}{\partial r} + \frac{1}{\sigma r}\hat{h} - 1 - \frac{1}{\sigma}\right), \tag{4.5}$$

$$\hat{v} = -\frac{1}{\sigma^2 - 1}\left(\frac{\partial \hat{h}}{\partial r} + \frac{\sigma}{r}\hat{h} - 1 - \sigma\right), \tag{4.6}$$

where

$$\hat{A} = \frac{1 + \frac{1}{\sigma} - i\frac{\alpha}{\sigma}}{J_1(s)\left[\left(1 - \frac{i\alpha}{\sigma}\right)\left(\frac{sJ_0(s)}{J_1(s)} - 1\right) + \frac{1}{\sigma}\right]},$$

$$s = \left\{\Delta\left[\sigma^2\left(1 - i\frac{\alpha}{\sigma}\right) - \left(1 - i\frac{\alpha}{\sigma}\right)^{-1}\right]\right\}^{1/2}.$$

Without friction this would be the solution of Lamb (1932, §211).

For the nonresonant case, the above solution can be expanded as

$$\hat{h} = AJ_1(kr) + i\alpha A\left[BJ_1(kr) - \frac{\sigma^2 + 1}{2\sigma(\sigma^2 - 1)}krJ_0(kr)\right] + O(\alpha^2), \tag{4.7}$$

where

$$A = \frac{1 + \frac{1}{\sigma}}{J_1(k)\left[\frac{kJ_0(k)}{J_1(k)} - 1 + \frac{1}{\sigma}\right]},$$

$$B = \frac{AJ_1(k)}{\sigma + 1}\left[\frac{kJ_0(k)}{J_1(k)}\frac{\sigma^3 + 3\sigma^2 - \sigma + 1}{2\sigma(\sigma^2 - 1)} - \frac{2}{\sigma + 1} - \frac{\Delta(\sigma^2 + 1)}{2}\right],$$

$$k = [\Delta(\sigma^2 - 1)]^{1/2}.$$

Since A and B are real, the frictional correction is purely imaginary. Thus, for small friction there is only a small phase shift with no amplitude change. But, exactly at resonance, the solution is

$$\hat{h} = \frac{i}{\alpha}CJ_1(kr) + O(1), \tag{4.8}$$

where

$$C = \frac{-(\sigma + 1)}{J_1(k)\left[\frac{\sigma^2 + 1}{2}\left(\Delta - \frac{1}{\sigma^2}\right) + \frac{1}{\sigma}\right]}.$$

Since $\hat{h}$ is purely imaginary, there is a 90° phase shift from the inviscid solution.

Having determined the effect of friction on the primary response, we now examine the inviscid forced problem. Fig. 4 shows resonance curves for the first three inviscid modes with azimuthal wavenumber 1, as a function of Δ. The resonance curves are the solid lines and the thick dashed lines separate the regions of dominant influence of neighboring modes. The resonance curves are lines where the amplitude of thermocline displacement at the coast changes from $+\infty$ to $-\infty$ in the direction of increasing $|\sigma|$, and lines that separate the region of dominant influence are drawn between resonance curves whenever this amplitude goes through zero. The phase of the forced response for each rotary component can then be determined by the region of influence it lies in, and the amplitude depends on its proximity to the resonance curves. The thin dashed lines are the nondimensional diurnal and semidiurnal frequencies for Lake Kinneret and the dots on these lines are based on an estimated Δ for the lake.

b. The secondary response

Taking the time average of the $O(\epsilon)$ equation of (2.3) and retaining terms to $O(\alpha_B, \alpha_I)$, we obtain

$$\langle \hat{\mathbf{k}} \times \mathbf{V} + \nabla h + \alpha_I \mathbf{V} - \alpha_B \mathbf{V}_2 \rangle_1 = -\frac{1 - 2\lambda}{1 - \lambda}\langle \mathbf{V}\cdot\nabla\mathbf{V}\rangle_0 - \Delta\langle h\mathbf{F}\rangle_0 - \langle \mathbf{V}\cdot\nabla\underline{\mathbf{V}} + \underline{\mathbf{V}}\cdot\nabla\mathbf{V}\rangle_0 + \Delta\left[\frac{\alpha_I(1 - 2\lambda)}{1 - \lambda} - \frac{\alpha_B\lambda^2}{(1 - \lambda)^2}\right]\langle h\mathbf{V}\rangle_0, \tag{4.9}$$

$$\langle \nabla\cdot\mathbf{V}\rangle_1 = -\frac{\Delta(1 - 2\lambda)}{(1 - \lambda)}\langle \nabla\cdot h\mathbf{V}\rangle_0 - \Delta\langle \nabla\cdot h\underline{\mathbf{V}}\rangle_0, \tag{4.10}$$

$$\langle \hat{\mathbf{k}} \times \underline{\mathbf{V}} + \nabla(\eta - h) + \alpha_B \mathbf{V}_2 \rangle_1 = -\frac{\lambda}{1 - \lambda}[\Delta\langle h\nabla h\rangle_0 + \langle \mathbf{V}\nabla\cdot\mathbf{V}\rangle_0 + \langle \mathbf{V}\cdot\nabla\mathbf{V}\rangle_0], \tag{4.11}$$

$$\langle \nabla\cdot\underline{\mathbf{V}}\rangle_1 = 0. \tag{4.12}$$

The vorticity equation for the barotropic component can be derived from (4.11) and (4.12):

$$\alpha_B \hat{\mathbf{k}}\cdot\nabla \times \langle \mathbf{V}_2\rangle_1 = -\frac{\lambda}{1-\lambda}\hat{\mathbf{k}}\cdot\nabla \times [\langle \mathbf{V}\nabla\cdot\mathbf{V}\rangle_0 + \langle \mathbf{V}\cdot\nabla\mathbf{V}\rangle_0]. \quad (4.13)$$

Since

$$\langle \mathbf{V}\nabla\cdot\mathbf{V}\rangle_0 = -\Delta\langle \mathbf{V}\partial h/\partial t\rangle_0 = \Delta\langle h\partial\mathbf{V}/\partial t\rangle_0$$
$$= -\Delta[\langle h\hat{\mathbf{k}}\times\mathbf{V}\rangle_0 - \langle h\mathbf{F}\rangle_0 + \alpha\langle h\mathbf{V}\rangle_0 + \tfrac{1}{2}\nabla\langle h^2\rangle_0],$$

we obtain

$$\hat{\mathbf{k}}\cdot\nabla \times \langle \mathbf{V}\nabla\cdot\mathbf{V}\rangle_0 = -\Delta\nabla\cdot\langle h\mathbf{V}\rangle_0 - \Delta\hat{\mathbf{k}}\cdot\nabla\times\langle h(\alpha\mathbf{V}-\mathbf{F})\rangle_0.$$

Also, it can easily be derived that

$$\hat{\mathbf{k}}\cdot\nabla \times \langle \mathbf{V}\cdot\nabla\mathbf{V}\rangle_0 = \nabla\cdot\langle\zeta\mathbf{V}\rangle_0,$$

where ζ is the baroclinic relative vorticity. Thus, (4.13) implies that

$$\alpha_B\hat{\mathbf{k}}\cdot\nabla\times\langle\mathbf{V}_2\rangle_1 = \frac{\lambda}{1-\lambda}[\nabla\cdot\langle(\Delta h-\zeta)\mathbf{V}\rangle_0 + \Delta\hat{\mathbf{k}}\cdot\nabla\times\langle\alpha h\mathbf{V}-\mathbf{F}h\rangle_0]. \quad (4.14)$$

This equation states that there is a balance between bottom friction, advection of baroclinic potential vorticity and nonlinear forcing caused by the feedback mechanism.

An equation similar to (3.6) can be derived by taking the azimuthal mean of the azimuthal component of Eq. (4.11); this gives

$$\alpha_B\overline{\langle v_2\rangle_1}^{\theta} = -\frac{\lambda}{1-\lambda}\left[\overline{\langle v\nabla\cdot\mathbf{V}\rangle_0}^{\theta} + \overline{\langle\mathbf{V}\cdot\nabla v\rangle_0}^{\theta} + \frac{1}{r}\overline{\langle uv\rangle_0}^{\theta}\right]$$
$$= -\frac{\lambda}{(1-\lambda)r^2}\frac{\partial}{\partial r}\overline{\langle r^2uv\rangle_0}^{\theta}.$$

Therefore,

$$\int_0^1 r^2\overline{\langle v_2\rangle_1}^{\theta}dr = 0. \quad (4.15)$$

Because of this, the lower layer mean longshore flow must have at least one reversal in direction.

Integrating (4.14) over the basin yields

$$\alpha_B\langle v_2\rangle_{1,c} = \frac{\Delta\lambda}{1-\lambda}[\alpha\langle hv\rangle_c - \langle hF^{\theta}\rangle_c]_0. \quad (4.16)$$

The angle brace $\langle\ \rangle_c$ implies an average over θ and t evaluated at the coast. Using this expression and the primary solution, we can determine the sign of lower layer flow at the coast.

Substituting (4.6) and (4.7) into (4.16) yields

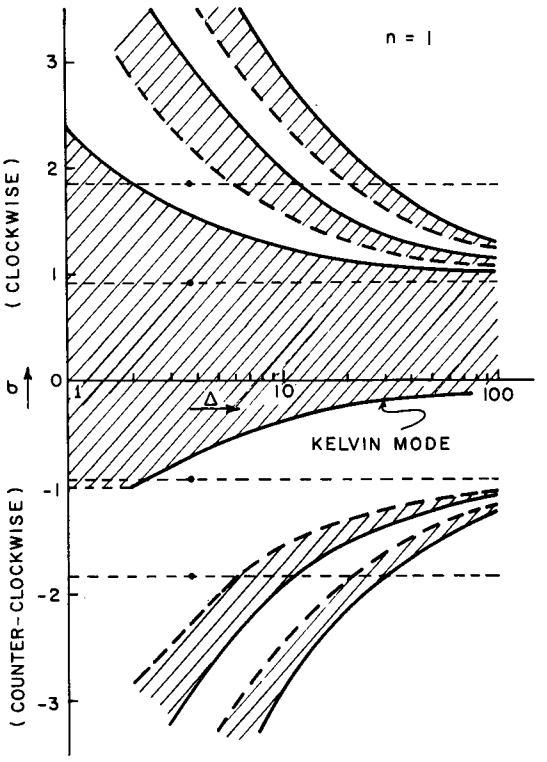

FIG. 4. First three inviscid modes (with azimuthal wavenumber 1) of a circular basin. Solid lines are resonance frequencies, and thick dashed lines separate regions of dominant influence of neighboring modes. Thin dashed lines represent diurnal and semidiurnal frequencies for Lake Kinneret, and the dots correspond to an estimate of Δ.

$$\langle v_2\rangle_{1,c} = \frac{\Delta(1+\delta\lambda^2)}{2\delta(1-\lambda)^2}\frac{A^2J_1^2(k)}{\sigma+1} \times\left\{\frac{kJ_0(k)}{J_1(k)}\left[-\frac{1}{\sigma-1}+\frac{(\sigma^2+1)}{2(\sigma^2-1)}\frac{kJ_0(k)}{J_1(k)}\right] - \frac{2\sigma}{\sigma+1}+\frac{\Delta(\sigma^2+1)}{2}\right\},$$

where δ is the ratio of bottom friction coefficient C_B to interface friction coefficient C_I.

In Fig. 5, we plot the sign of $\langle v_2\rangle_{1,c}$ as a function of σ and Δ. The net flow, which is the sum of the two rotary components, is cyclonic when the forcing frequency is lower than the critical frequency shown by the solid curve. Since the resonant frequency of the Kelvin mode is lower than this critical frequency, we conclude that the lower layer flow at the coast is generally cyclonic if the Kelvin mode is the dominant mode that is excited.

By a similar procedure, we can form the vorticity equation for the baroclinic mode from (4.9) and (4.10):

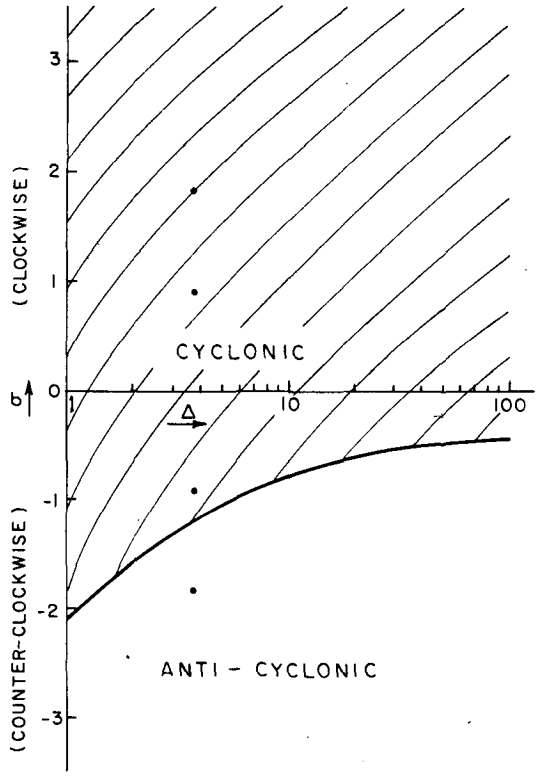

FIG. 5. The sign of the mean lower layer flow at the coast, $\langle v_2\rangle_{1,c}$ as a function of frequency σ and Δ. The solid dots are estimates for Lake Kinneret.

$$\alpha_I\hat{\mathbf{k}}\cdot\nabla\times\langle\mathbf{V}\rangle_1=\nabla\cdot\langle(\Delta h-\underline{\zeta})\mathbf{V}\rangle_0+\Delta\hat{\mathbf{k}}\cdot\nabla\times\langle\alpha_I h\mathbf{V}-\frac{1}{1-\lambda}h\mathbf{F}\rangle_0, \quad (4.17)$$

where $\underline{\zeta}$ is the barotropic relative velocity. Integrating over the basin gives

$$\alpha_I\langle v\rangle_{1,c}=\Delta\left[\alpha_I\langle hv\rangle_c-\frac{1}{1-\lambda}\langle hF^\theta\rangle_c\right]_0. \quad (4.18)$$

Substituting (4.6), (4.7) into (4.18) yields

$$\langle v\rangle_{1,c}=\frac{\Delta A^2J_1^2(k)}{2(\sigma+1)}\left\{\frac{kJ_0(k)}{J_1(k)}-2-\frac{1+\delta\lambda^2}{1-\lambda}\times\left[\frac{kJ_0(k)}{J_1(k)}\left(\frac{\sigma}{\sigma-1}-\frac{\sigma^2+1}{2(\sigma^2-1)}\frac{kJ_0(k)}{J_1(k)}\right)-\frac{2}{\sigma+1}-\frac{\Delta(\sigma^2+1)}{2}\right]\right\}. \quad (4.19)$$

The sign of this depends not only on σ and Δ, as does $\langle v_2\rangle_{1,c}$, but also on λ and δ. Hence, no simple conclusion can be made for the general case. But, for the special case when the resonance condition for the Kelvin mode is satisfied, we derive, from (4.6), (4.8) and (4.18), that

$$\alpha_I\langle v\rangle_{1,c}=\frac{\Delta\lambda^2}{(1-\lambda)(1+\delta\lambda^2)}\times\frac{(1+\sigma)}{2\alpha\Gamma}(\delta-\delta_c), \quad (4.20)$$

where

$$\Gamma=\frac{1+\sigma^2}{2}\left(\Delta-\frac{1}{\sigma^2}\right)+\frac{1}{\sigma}$$

$$\delta_c=-\frac{1}{\lambda^2}\left[1-\frac{(1-\lambda)\left(1+\frac{1}{\sigma}\right)}{\Gamma}\right].$$

Since Γ is negative except for the small Δ limit where the frequency of the free Kelvin wave is greater than f, whenever $\delta<\delta_c$, $\langle v\rangle_{1,c}$ is positive. In Fig. 6, we plot the value of δ_c as a function of Δ and λ. Since δ_c decreases as λ increases, there is an anticyclonic baroclinic mean flow for large enough λ or δ. If we define λ_c as the value of λ where δ_c vanishes, then λ_c is the critical value above which no cyclonic baroclinic mean flow is possible for any δ. It can be seen that $\lambda_c\approx\frac{1}{3}$ for $\Delta=2$, and approaches the straight coast limit, 0.5, as Δ approaches infinity.

Also, from (4.9) at resonance,

$$\langle\partial h/\partial r\rangle_{1,c}=\langle v\rangle_{1,c}+\frac{1-2\lambda}{1-\lambda}\langle v^2\rangle_{0,c} \quad (4.21)$$

and from 4.5,

$$\langle h\rangle_{1,c}=-\sigma\langle\partial h/\partial r\rangle_{1,c}=|\sigma|\langle\partial h/\partial r\rangle_{1,c}. \quad (4.22)$$

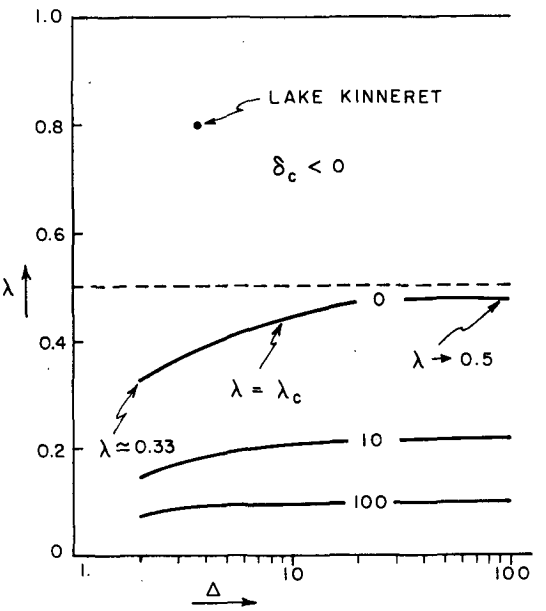

FIG. 6. The critical value of δ, the ratio of bottom to interface friction, as a function of λ, the ratio of thermocline depth to lake depth, and Δ the square of the ratio of the internal radius of deformation to the lake radius, for a resonant Kelvin wave.

From these two equations a definite conclusion about the sign of $\langle h\rangle_{1,c}$ and $\langle \partial h/\partial r\rangle_{1,c}$ can be stated for two conditions:

(i) If $\lambda \geq \frac{1}{2}$ and $\langle v\rangle_{1,c} < 0$, then $\langle h\rangle_{1,c}, \langle \partial h/\partial r\rangle_{1,c} < 0$.

(ii) If $\lambda \leq \frac{1}{2}$ and $\langle v\rangle_{1,c} > 0$, then $\langle h\rangle_{1,c}$ and $\langle \partial h/\partial r\rangle_{1,c} > 0$.

By referring to Fig. 6, we can then conclude as follows:

1) For $\lambda \geq \frac{1}{2}$, the values of $\langle v\rangle_{1,c}$, $\langle h\rangle_{1,c}$ and $\langle \partial h/\partial r\rangle_{1,c}$ are all negative. In other words, whenever the mean thermocline is deeper than half the total depth, there is an anticyclonic baroclinic flow and an upwelling at the coast.

2) For $\langle v\rangle_{1,c} > 0$, the values of $\langle h\rangle_{1,c}$ and $\langle \partial h/\partial r\rangle_{1,c}$ are both positive. Thus, a cyclonic baroclinic flow is always accompanied by a downwelling at the coast.

The existence of this critical value of λ can be understood by examining (4.18) more closely. The sign of $\langle v\rangle_{1,c}$ depends on the net effect of the feedback mechanisms associated with thermocline stress and surface stress, respectively. For a resonant Kelvin wave, the one associated with the thermocline stress always tends to induce a positive value since the longshore flow is essentially geostrophic and the amplitude of thermocline displacement decreases monotonically away from shore. In contrast, the one associated with the surface stress always tends to induce a negative value due to the positive correlation between v and F^{θ} required to maximize the energy input at resonance. The latter, being dependent on $\alpha/(1-\lambda)$, would dominate the response as δ or λ increases. Therefore, we eventually would get an anticyclonic baroclinic flow at the coast when δ or λ is large enough. Since δ_c slopes steeply except near λ_c, the direction of $\langle v\rangle_{1,c}$ is not very sensitive to the variation of δ except when λ is close to λ_c.

In summary, we conclude that the lower layer flow is cyclonic near the coast when the forcing frequency is lower than some critical value. For the special case of a resonant Kelvin mode, it was found that if δ (the ratio of bottom friction coefficient to interface friction coefficient) is smaller than some critical value δ_c, there is a cyclonic vertical shear. The critical curve of λ (the ratio of thermocline depth to total depth), above which no cyclonic vertical shear is possible, was also determined. It has the value of approximately $\frac{1}{3}$ for Δ of 2, and approaches $\frac{1}{2}$ as Δ approaches infinity. Most of these conclusions are strictly valid only for a resonant internal Kelvin wave; although internal Kelvin waves are observed in many lakes, the resonance condition is best satisfied by Lake Kinneret.

5. Application to Lake Kinneret

All observations in this section are from Serruya (1975); but anyone interested in a more general description of the meteorology, hydrology and limnology of Lake Kinneret should read Serruya's (1978) book. Lake Kinneret (Fig. 7) is located between 32°45′ and 32°55′N latitude; the inertial period is approximately 22 h. C, I, F and K are four mooring stations roughly equally spaced around the basin, and BB is a weather station. Fig. 8 shows the hourly wind averaged over the period 15–31 July 1971. There is a daily westerly that reaches its peak at about 1500 local time. Fig. 9 shows the wind and temperature data at the four stations K, C, I,

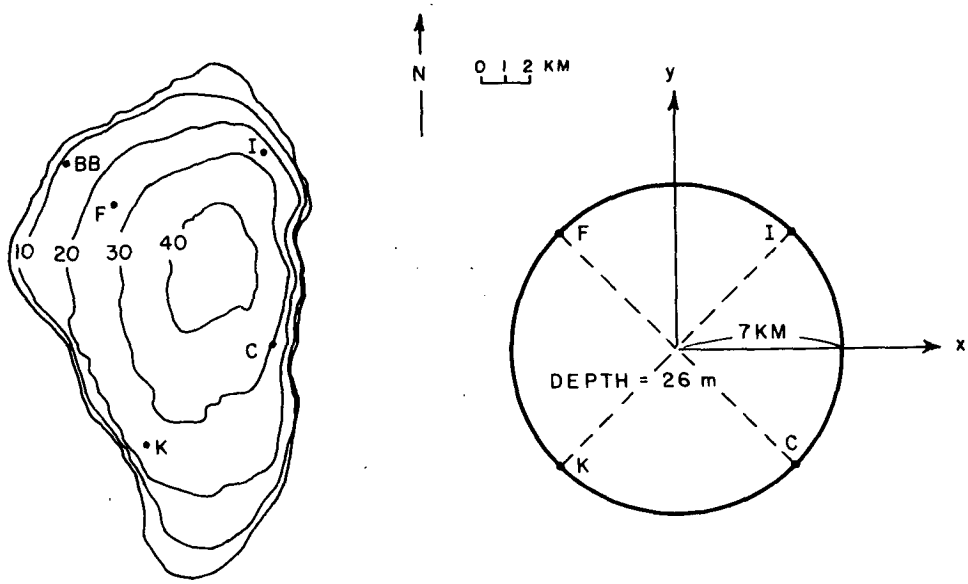

FIG. 7. Lake Kinneret and a model of Lake Kinneret. The depth contours are in meters.

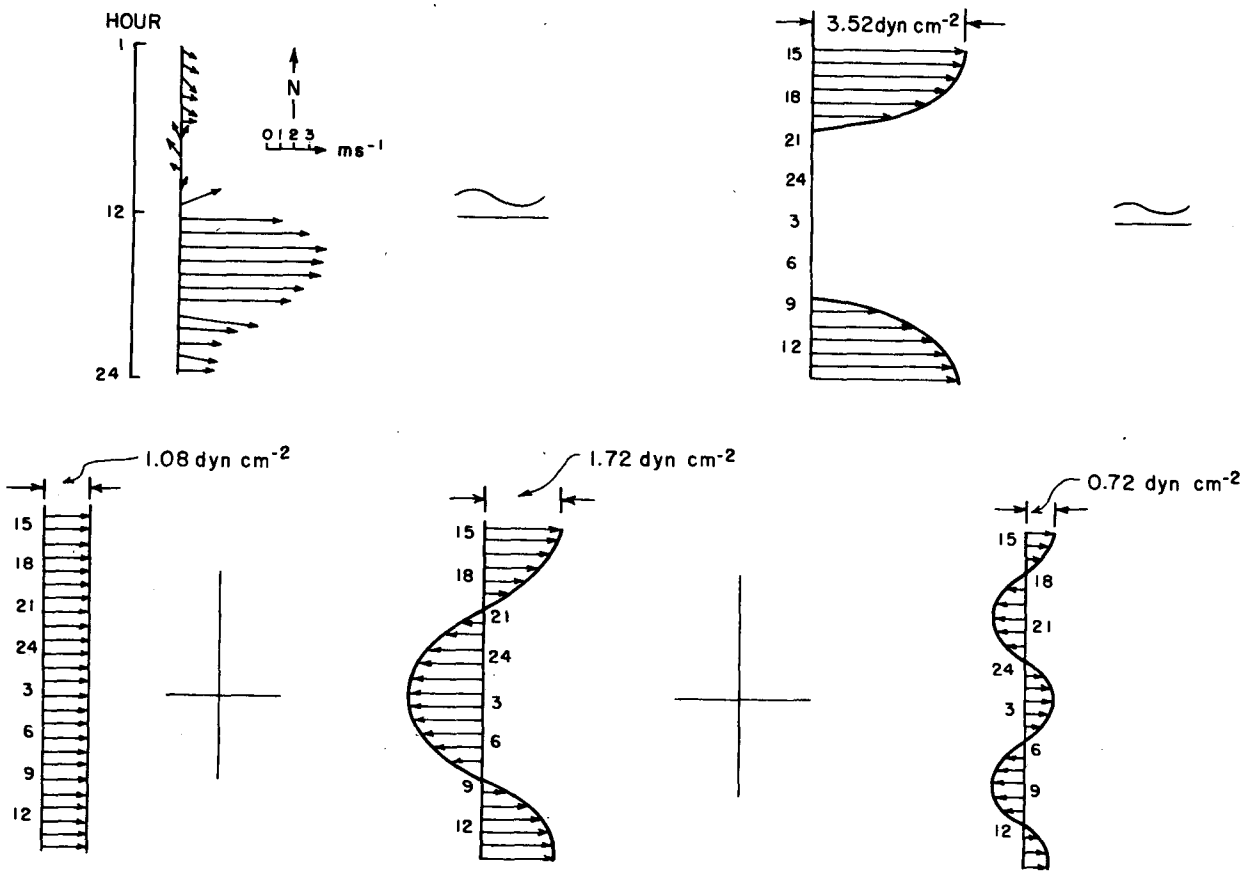

FIG. 8. Hourly winds averaged over 15–31 July 1971, the approximate stress, and its Fourier decomposition.

F during the period 14–20 July 1973. By graphical averaging, we estimated the diurnal and semidiurnal responses also shown in Fig. 9. The diurnal response is clearly a counterclockwise propagating wave; the semidiurnal response is more difficult to interpret, but it looks like a standing mode, with a nodal line in the north-south direction.

Fig. 10 shows progressive vector diagrams and the time average for currents at 3.5 and 21 m at the four stations during 1–5 June 1973. At both levels the flow is cyclonic but the speed is much higher near the surface.

Fig. 11 shows the depth of the thermocline obtained by Serruya from synoptic cruises of several times over a 3-day period. From this we can see that the patterns are roughly periodic with the maximum downwelling occurring in early morning in the northeast corner. The northwest corner, however, is clearly a region of upwelling at nearly all times.

Can the observations be explained by the model? To test this, we consider the circular model lake of Fig. 7. The radius is 7 km, the mean depth is 26 m, and the thermocline, roughly the 21°C isotherm, has a mean depth of 20 m. The wind, approximated by the half-cosine shape of Fig. 8, is composed of approximately 30% mean, 50% diurnal component and 20% semi-diurnal component. The density difference between the upper and lower layer is approximately 2×10^{-3} g cm^{-3}. This gives a reduced gravity of 1.96 cm s^{-2} and a Δ of 3.75. The ratio of the diurnal frequency to the inertial frequency is $\sim$0.922. These parameter values are represented by solid dots in Figs. 4–6. Due to the high phase uncertainty of the semi-diurnal component and its relative minor contribution to the secondary response, we will only discuss the diurnal component.

From the frictionless theory of Fig. 4 we expect the primary response to propagate counterclockwise and the upwelling to occur at the *downwind* shore—opposite what one would expect for steady flow. For this wave, which looks essentially like a resonant Kelvin wave, friction causes a phase shift which tends to make the upwelling occur at the shore to the left of the wind so that the longshore surface current is in phase with the wind, and the energy input is thus maximized. Thus, at the time of the peak westerly wind, 1500 LT, the upwelling should be maximum near the north shore. This is in agreement with the temperature observations of Fig. 9; at the time of the maximum wind speed the coldest water occurs between stations I and F.

According to Fig. 5, this diurnal component

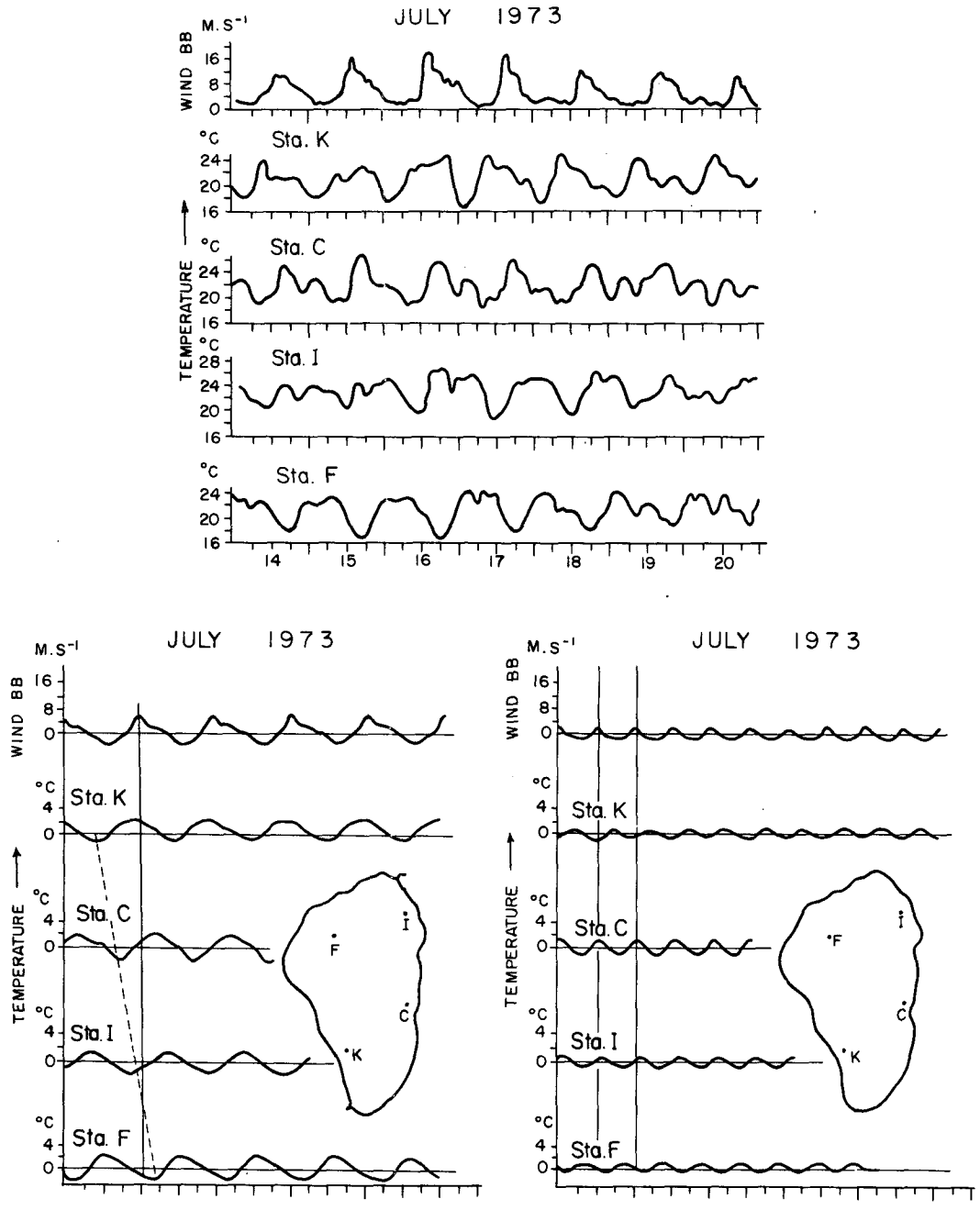

FIG. 9. Serruya's (1975) wind and temperature data, and its graphical decomposition into diurnal and semidiurnal components.

should generate a cyclonic lower layer flow at the coast. This agrees with the observations. The theory also predicts an anticyclonic mean drift somewhere in the interior region so that the net torque is zero. No observation is available to check this prediction.

We computed the baroclinic mean flow and thermocline slope for the parameters of Lake Kinneret. Because the dominant primary response is the Kelvin wave, they do not differ substantially from what one can conclude from Fig. 6 which assumes that the resonance condition for the Kelvin wave is satisfied. The value $\lambda = 0.8$ for this model lake is well above the critical curve of λ_c; we therefore expect an anticyclonic mean baroclinic flow and upwelling at the coast. This latter prediction, combined with the set up due to the mean wind component, may explain the relatively intense mean upwelling in the northwest corner of the lake shown in Fig. 11. The prediction of a mean anticyclonic baroclinic flow at the coast, however, disagrees with

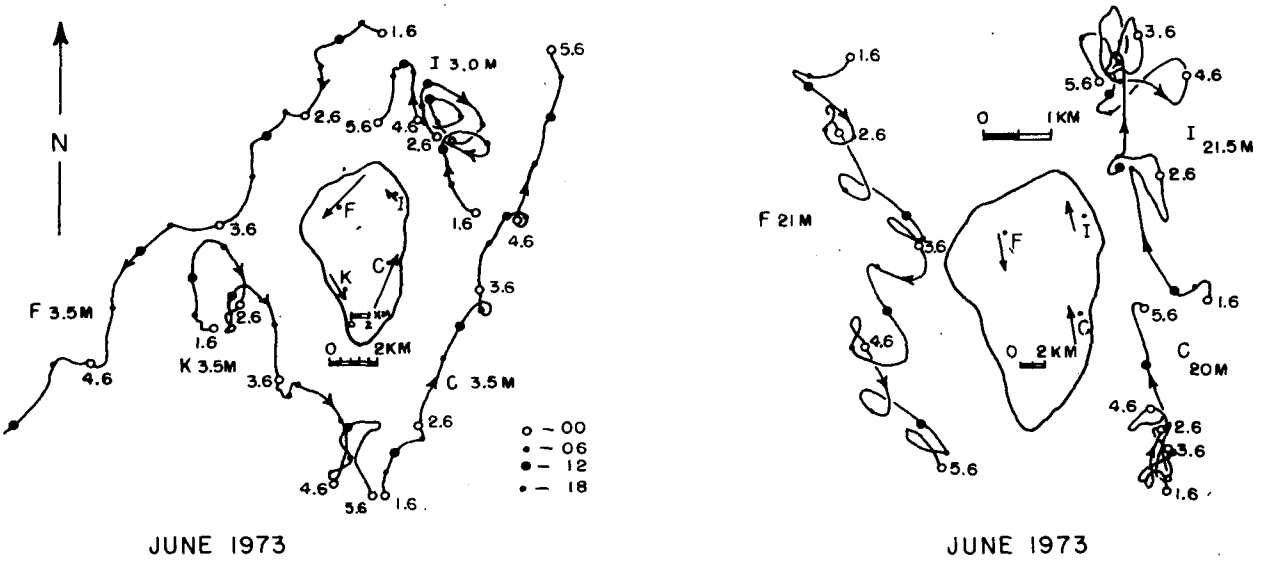

FIG. 10. Serruya's progressive vector diagrams and mean currents during 1–5 June 1973. Note that for the near-surface measurements on the left, the scales are different from the deeper measurements on the right; the surface currents are faster than the deeper currents.

the observations in Fig. 10. In Section 6 we show that adding topography improves this aspect of the theory.

6. Numerical calculations

As in the analytical theory, the primary response is assumed to be governed by the linear equations and the secondary response is driven by the nonlinear interactions of the primary variables. All the variables are expressed as

$$h(r,\theta,t) = h_1(r,t) + h_2(r,t)\sin\theta + h_3(r,t)\cos\theta + h_4(r,t)\sin 2\theta + h_5(r,t)\cos 2\theta. \quad (6.1)$$

The numerical model of Bennett (1978) was used to calculate the solutions presented here. Because the wind is uniform, the primary response is the $\sin\theta$ and $\cos\theta$ components, and the secondary response is the mean and the $\sin 2\theta$ and $\cos 2\theta$ components. The model was run with a periodic wind until a statistically steady state is reached, then averaged over one wave period to obtain the mean secondary response. The thermocline friction coefficient c is 0.005 cm s^{-1} and the bottom friction coefficient d is 0.02 cm s^{-1}.

At the top of Fig. 12 is the mean thermocline displacement and streamfunction induced by the diurnal wind for a uniform depth of 26 m and a mean thermocline depth of 20 m. As predicted by the analytical theory there is a mean upwelling of the thermocline at the coast and a cyclonic circulation. The higher harmonic structure is caused by correlation of the two oppositely propagating primary waves. At the bottom of Fig. 12 is the solution for a parabolic bottom with a minimum depth at the shore of 20 m, a mean thermocline depth of 15 m and a maximum depth of 50 m. Notice that the coastal upwelling zone of the flat bottom lake is pushed offshore while an apparent downwelling is induced at the coast. This downwelling implies a cyclonic vertical shear. This result agrees with the observations better than the constant depth case because the observed flow is much stronger above

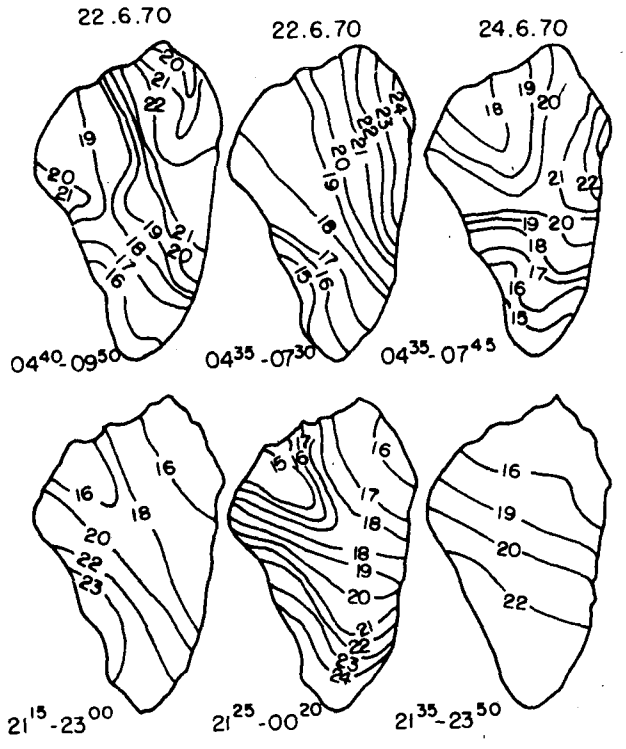

FIG. 11. Serruya's maps of thermocline depth (m) measured twice a day, 22–24 June 1976.

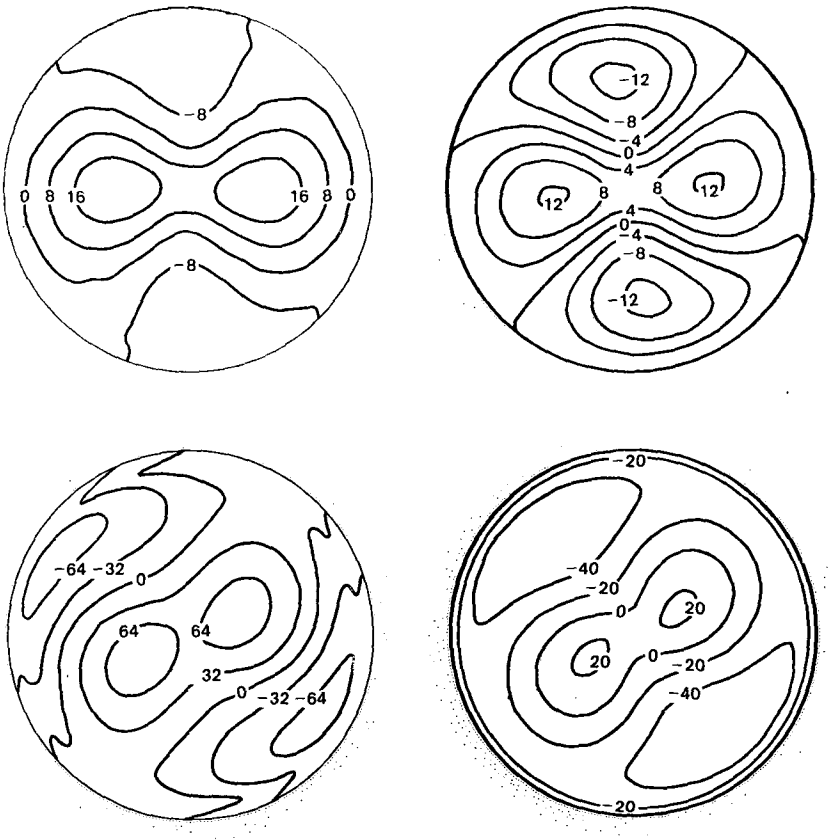

FIG. 12. Thermocline displacement (cm), negative values implying upwelling, and transport streamfunction (10^8 cm^3 s^{-1}) numerically calculated for a model of Lake Kinneret. At the top is the solution for a constant depth; at the bottom is the solution for a parabolic bottom.

the thermocline. The magnitude of the flow is also more reasonable—the maximum upper layer current in this model is ~8 cm s^{-1}. Finally, the maximum current speed occur in approximately the correct spots, the northwest and southeast corners.

It is reasonable that this large variation of depth can cause such a radically different solution, but the reason for it is not clear. Bennett (1978) found, for Lake Ontario, that rectification of topographic waves was important. However, this cannot be the case here because the topographic waves for this model have periods of about a week and are not resonantly excited by the diurnal wind. It seems more likely that the depth variation influences the solution in causing friction to be more effective in the shallow nearshore region than offshore. It would clearly be worthwhile to extend the analytical theory to a case of variable depth.

Acknowledgments. We thank D. B. Rao for his comments. This work was supported at the Massachusetts Institute of Technology by Brookhaven National Laboratory under Contract 357213-S, by the Great Lakes Environmental Research Laboratory of the National Oceanic and Atmospheric Administration under Contract 03-022-57, and at the Woods Hole Oceanographic Institution by the National Science Foundation under Grant OCE 76-01813.

REFERENCES

Bennett, J. R., 1973: A theory of large-amplitude Kelvin waves. *J. Phys. Oceanogr.*, **3,** 57–60.

——, 1978: A Three-dimensional model of Lake Ontario's summer circulation. II. A diagnostic study. *J. Phys. Oceanogr.*, **8,** 1095–1103.

Emery, K. O., and Csanady, G. T., 1973: Surface circulation of lakes and nearly land-locked seas. *Proc. U.S. Nat. Acad. Sci.*, **70,** 93–97.

Lamb, H., 1932: *Hydrodynamics,* 6th ed. Cambridge University Press, 738 pp.

Longuet-Higgins, M. S., 1969: On the transport of mass by time varying ocean currents. *Deep-Sea Res.*, **16,** 431–448.

Serruya, C., Ed. 1978: *Lake Kinneret.* Junk, 501 pp.

Serruya, S., 1975: Wind, Water Temperature and motions in Lake Kinneret: General pattern. *Ver. Int. Verein. Limnol.*, **19,** 73–87.

Thompson, R., 1970: Diurnal tides and shear instabilities in a rotating cylinder. *J. Fluid Mech.*, **40,** 737–751.

Wunsch, C. I., 1973: On the mean drift in large lakes. *Limnol. Oceanogr.*, **18,** 793–795.